

# Signatures of spin pairing in a quantum dot in the Coulomb blockade regime

S. Lüscher<sup>1</sup>, T. Heinzel<sup>1</sup>, K. Ensslin<sup>1</sup>, W. Wegscheider,<sup>2,3</sup> and M. Bichler<sup>3</sup>

<sup>1</sup>*Solid State Physics Laboratory, ETH Zürich, 8093 Zürich, Switzerland*

<sup>2</sup>*Institut für Angewandte und Experimentelle Physik, Universität Regensburg, 93040 Regensburg, Germany*

<sup>3</sup>*Walter Schottky Institut, TU München, 85748 Garching, Germany*

(November 11, 2018)

Coulomb blockade resonances are measured in a GaAs quantum dot in which both shape deformations and interactions are small. The parametric evolution of the Coulomb blockade peaks shows a pronounced pair correlation in both position and amplitude, which is interpreted as spin pairing. As a consequence, the nearest-neighbor distribution of peak spacings can be well approximated by a smeared bimodal Wigner surmise, provided that interactions which go beyond the constant interaction model are taken into account.

PACS numbers: 73.20.My, 73.23.Hk, 05.45.+b

Recently, the Coulomb blockade (CB) of electronic transport through quantum dots, defined in two-dimensional electron gases in semiconductor heterostructures, has been of considerable interest [1]. One reason is that such dots are model systems to investigate the interplay between chaos and electron-electron (e-e) interactions. Here, a key feature is the distribution of nearest-neighbor Coulomb blockade peak spacings (NNS), which random matrix theory [2] (RMT) predicts to follow a bimodal Wigner surmise  $P(s)$  for a non-interacting quantum dot of chaotic shape, i.e.

$$P(s) = \frac{1}{2} [\delta(s) + P^\beta(s)] \quad (1)$$

$P^\beta(s)$  is the Wigner surmise for the corresponding Gaussian ensemble, i.e.  $\beta = 1$  for systems with time inversion symmetry (Gaussian orthogonal ensemble - GOE), and  $\beta = 2$  when time inversion symmetry is broken (Gaussian unitary ensemble - GUE). The peak spacing  $s$  is measured in units of the average spin-degenerate energy level spacing  $\Delta = 2\pi\hbar^2/(m^*A)$ , where  $m^*$  denotes the effective mass, and  $A$  the dot area. The  $\delta$ -function in  $P(s)$  takes the spin degeneracy into account. RMT further predicts the standard deviation for  $P(s)$  to be  $\sigma = 0.62$  for  $\beta = 1$ , and  $\sigma = 0.58$  for  $\beta = 2$ , respectively [3].

The comparison to experimental data is made by applying the constant-interaction model [4,5], which allows to separate the constant single-electron charging energy from the fluctuating energies of the levels inside the dot. In disagreement with the predictions of RMT, the experimentally obtained NNS distributions are usually best described by a *single Gaussian* with enhanced values of  $\sigma$  [6–9]. The data thus look as if spins are absent, although in Ref. [10], a spin pair has been observed. This apparent absence of spins and the different shape of  $P(s)$  have triggered tremendous recent theoretical work. One possible explanation are additional e-e interactions inside the dot [6,11–16], which lead to “scrambling” of the energy spectrum [17,10] and can be characterized by the interaction parameter  $r_s$ , defined as the ratio between

the Coulomb interaction of two electrons at their average spacial separation, and the Fermi energy [11,14–16]. It is theoretically expected that the NNS distribution becomes Gaussian due to e-e interactions, and that  $\sigma$  increases for  $r_s \geq 2$ . [14,15]. However, all experiments so far have been carried out in a regime where an increase in  $\sigma$  is not expected, i.e. in samples with  $0.93 \leq r_s \leq 1.35$  [6–8], with the exception of Ref. [9], where  $r_s = 2.1$ . Gate-voltage induced shape deformations of the dot can modify the NNS distribution as well. The deformation can be described by a parameter  $x$ , which corresponds to the distance between avoided crossings induced by the deformation, measured in units of the CB peak spacing. For  $x \approx 1$ , the NNS distribution of partly uncorrelated energy spectra is measured, resulting again in a Gaussian shape with enhanced  $\sigma$  [18,19]. Whether shape deformations or interactions dominate the shape of the NNS distribution is not clear, although there is experimental evidence that  $x < 1$  and interactions are more important [9,10].

Here, we report measurements on a quantum dot in which shape deformations as well as  $r_s$  are reduced. We observe a pronounced pairwise correlation of both position and amplitude of the Coulomb blockade resonances, which is sometimes interrupted by kinks in the parametric evolution, among other features. We interpret the pairing as a spin signature: the energies of two states belonging to the same spatial wave function with opposite spin differ by an average interaction energy  $\bar{\xi}$ , which fluctuates with a standard deviation of  $\sigma_\xi$ , both of which are of the order of  $\Delta$ . We conclude that in previous experiments, spin pairing was difficult to observe because it was frequently destroyed by avoided level crossings. Furthermore, we suggest that the measured NNS distribution can be fitted to a modified bimodal Wigner surmise, with  $\bar{\xi}$  and  $\sigma_\xi$  as fit parameters.

The sample is a shallow Ga[Al]As heterostructure with a two-dimensional electron gas (2DEG) 34 nm below the surface. The quantum dot is defined by local oxidation with an atomic force microscope [20] (inset in Fig.1(a)).

The lithographic dot area is 280 nm x 280 nm. The dot can be tuned by voltages applied to a homogeneous top gate and to the planar gates I and II. In order to reduce  $r_s$  as much as possible, we chose a heterostructure with a high electron density, further increased by a top gate voltage of +100 mV to  $n_e = 5.9 \cdot 10^{15} \text{ m}^{-2}$ . This results in  $r_s = 0.72$ , which is smaller than in all previous experiments. Additional screening is provided by the top gate [21]. The sample was mounted in the mixing chamber of a  $^3\text{He}/^4\text{He}$ -dilution refrigerator with a base temperature of 90 mK. The mobility of the cooled 2DEG was 93  $\text{m}^2/\text{Vs}$ . A DC bias voltage of 10  $\mu\text{V}$  was applied across the dot, and the current is measured with a resolution of 500 fA. From capacitance measurements [5], we find the electronic dot area  $A=190 \text{ nm} \times 190 \text{ nm}$  (the depletion length in such devices can be smaller than in structures defined by top gates [20]). The single-electron charging energy is  $E_c = 1.25 \text{ meV}$  and the spin-edgdegenerate level spacing  $\Delta = 200 \mu\text{eV}$ .

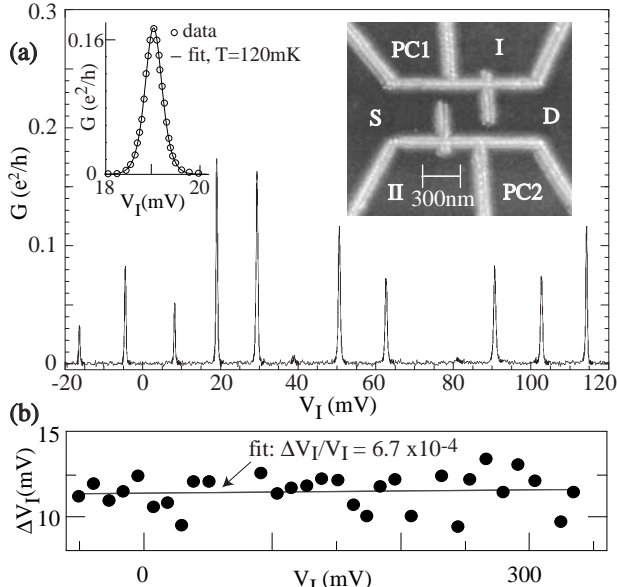


FIG. 1. (a) Right inset: AFM picture (taken before evaporation of the top gate) of the oxide lines (bright) that define the dot, coupled to source (S) and drain (D) via tunnel barriers, which can be adjusted with the planar gates PC1 and PC2. Gates I and II are used to tune the dot. Main figure: Conductance  $G$  as a function of  $V_I$ , showing Coulomb blockade resonances. Left inset: fit (line) to one measured CB peak (open circles), see text. (b) Linear fit (line) of the peak spacing  $\Delta V_I$  as a function of  $V_I$  (dots). The average peak spacing is almost constant, indicating small shape deformations.

The measurements have been carried out in the weak coupling regime,  $\hbar\Gamma \ll k_B T \ll \Delta$ . Here,  $\Gamma$  denotes the coupling of the dot to source and drain. The conductance  $G$  was measured as a function of the voltage  $V_I$  applied to the planar gate I (see inset in Fig. 1(a)). Magnetic fields  $B$  applied perpendicular to the sample surface and  $V_{II}$  were used as parameters. The observed CB

oscillations (Fig. 1(a)) are fitted to a thermally broadened line shape, i.e.,  $G(V_I) = G_{max} \cosh^{-2}(\eta V_I / 2k_B T)$  [4], yielding an electron temperature of  $T=120\text{mK}$ , as well as the positions and amplitudes of the peaks. Here,  $\eta = 0.11\text{eV}/V$  is the lever arm. Fig. 1 (b) shows the peak spacing  $\Delta V_I$  as a function of  $V_I$ . Compared to conventional dots defined by top gates, we find a much smaller variation of the average peak spacing as  $V_I$  is tuned, although the fluctuation of individual spacings is 15% of  $E_c$ . A linear fit gives a slope of  $\Delta V_I/V_I = 6.7 \cdot 10^{-4}$ . Hence, the capacitance between the dot and gate I varies only by 3% over the whole scan range, as compared to, for example, a factor of 3 in Ref. [7]. This indicates that tuning gate I or II predominantly changes the energy of the conduction band bottom, while the dot is only slightly deformed. By applying the method of Ref. [18] to a hard-wall confinement, we estimate  $x \approx 0.15$  for our dot as a lower limit.

In Fig. 2 (a), five consecutive CB peaks are shown as a function of  $B$ . A pronounced pairwise correlation of both amplitude and peak position is observed (peak b correlates with peak c, and peak d with peak e, respectively). Observation of a pairing has been reported previously and interpreted as spin pairing [10], but not been further investigated.

We interpret this parametric pair correlation in terms of a model recently developed by Baranger et al. [22]. The constant interaction model is used to subtract  $E_c$  from the peak spacings. The remaining individual energy separations equal  $\Delta/2$  on average and reflect the fluctuating level separations inside the quantum dot, which consist of two parts. We assume that two paired peaks belong to the same spatial wave function, labelled by  $i$ , of opposite spin, and are split by an interaction energy  $\xi_i$ , while the energy of consecutive states with different orbital wave functions differs by  $\Delta_i - \xi_i$ . Since the separations between the two levels of equal spin of spin pair  $i$  and  $(i+1)$ ,  $\Delta_i$ , and possibly also  $\xi_i$ , vary as a function of  $B$ , levels may cross and the ground state of the dot can be either a singlet or a triplet state. At the singlet-triplet transitions, kinks in the parametric peak evolution occur and the pair correlation is interrupted [22]. We can identify such kinks in our data, among other features. Fig. 2 (b) shows the amplitudes of peaks c, d and e. The correlation between peaks d and e is very strong around  $B=0$ . For  $0.4T < B < 0.61T$ , this correlation is interrupted, while the amplitudes of peaks c and e are correlated instead. In this regime, correlated kinks in the evolution of peaks c and d are observed (Fig. 2 (c)). In Fig. 2 (d), a possible corresponding scenario for the parametric dependence of energy levels is sketched: (left) two avoided crossings occur between level pair  $i$  and level pair  $i+1$ . This leads to the position of peaks c, d, and e as sketched in Fig. 2 (d), right, corresponding to the difference in energy upon changing the electron number in the dot. Consequently, positions and amplitudes of peaks c and e should be cor-

related in  $0.4T < B < 0.61T$ , as observed. Note that this correlation is interrupted around  $B=0.5T$ , possibly due to the influence of another energy level.

Also,  $\xi_{de}$  is not constant over the full range of  $B$ . While  $\xi_{de} \approx 0.05\Delta$  for  $B < 0.22T$ , the positions of peaks d and e are not detectable in  $0.22T < B < 0.32T$ , since their amplitudes vanish. As the peaks reappear,  $\xi_{de}$  has jumped to  $\xi_{de}^* \approx 0.25\Delta$ . We speculate that possibly a level crossing has occurred in the regime where the amplitudes are suppressed, and hence for  $B < 0.22T$ , a different level pair is at the Fermi energy than for  $B > 0.32T$ . In addition, we note that although  $\xi$  fluctuates as  $B$  is varied, a systematic change of  $\xi$  with  $B$  is not observed, which indicates that Zeemann splitting plays a minor role. From the data of Fig. 2, we estimate the average interaction energy to  $\bar{\xi} \approx 0.5\Delta$  by averaging over all peaks and magnetic fields. Baranger et al. have estimated  $\bar{\xi} \approx 0.6\Delta$  for  $r_s = 1$ . Hence, our findings can be considered as being in agreement with existing theory, while we are not aware of a theoretical prediction for  $\sigma_\xi$ . From the above phenomenology, we conclude that for dots with stronger shape deformations, and hence more level crossings, or in dots with larger  $r_s$  (and thus larger  $\bar{\xi}$ ), the spin pairing is frequently interrupted and difficult to detect. Also, the Kondo effect [23] can occur in neighboring peaks [24] when spin pairing is interrupted.

We proceed by discussing the effect of spin pairing on the NNS distributions. In Fig. 3, the measured histograms of the normalized NNS distributions for GOE (a) and GUE (b) are shown. The ensemble statistics have been obtained by measuring  $G(V_I)$ , and either by changing the magnetic flux by one flux quantum  $\phi_o = \frac{\hbar}{e}$  through the dot (GUE), or by stepping  $V_{II}$  in units of one CB period (GOE). Each individual  $V_I$ -sweep contains 15 CB resonances in the low coupling regime. The total number of peak spacings used is 120 for GOE, and 210 for GUE, respectively. The individual level spacings  $s$  in units of  $\Delta$  are obtained by using the fit of Fig. 1b; its expectation value is  $\bar{s}=0.5$ . Both histograms are asymmetric and show no evident bimodal structure. By including the effect of spin pairing into the statistics, however, we can interpret them as modified bimodal distributions:

- (i) The  $\delta$ -function in the non-interacting NNS distribution  $P(s)$  with the expectation value of  $\bar{s}_\delta=0$  (eq. (1)) is shifted to  $\bar{s}_\delta = \bar{\xi}^*$  and, as a reasonable assumption [25], broadened according to a Gaussian distribution with the standard deviation  $\sigma_{\xi^*}$ . Here,  $\xi^*$  denotes the interaction energy in units of  $\Delta$ .
- (ii) Since one level of a spin pair  $i$  is shifted upwards in energy by  $\xi_i$ , the separation between the upper level of spin pair  $i$  and the lower level of pair  $(i+1)$  is given by  $\Delta_{i+1} - \xi_i$ . Consequently,  $P^\beta(s)$  in eq. (1) is shifted to  $\bar{s}_{P^\beta} = 1 - \xi^*$  and convoluted with the Gaussian distribution function of  $\xi^*$ .

Combining these two components, the modified NNS distribution reads

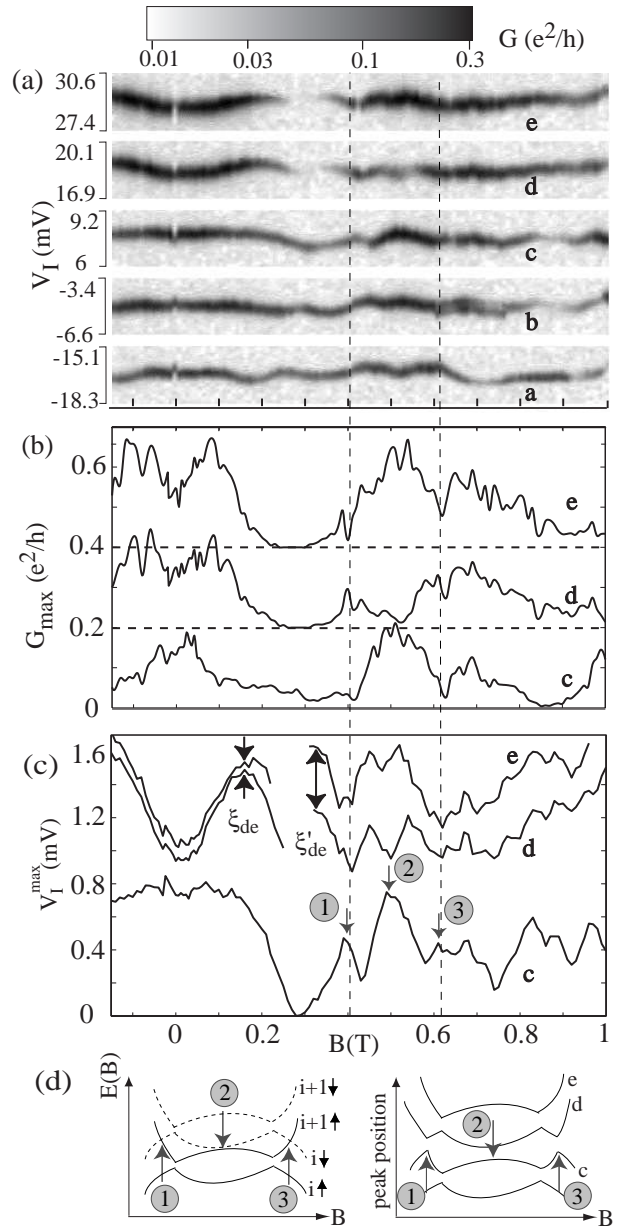


FIG. 2. (a) Logarithmic grayscale plot of parametric variations in a magnetic field  $B$  for 5 consecutive CB peaks. A pair correlation in peak position amplitude is observed, which is interrupted in certain ranges of  $B$ , for example in the region between the dashed lines. (b) Parametric amplitudes for peaks c, d, and e, offset by  $0.2 e^2/h$  each. The correlation between peak d and e is lost in  $0.4T < B < 0.6T$ , and e correlates with c instead. (c) The corresponding position of the peak maxima. The traces are offset for clarity. At magnetic fields labelled by 1 and 3, kinks in the peak position occur, while the separation between peak d and e jumps across the region of suppressed amplitude from  $\xi_{de}$  to  $\xi'_{de}$ . (d) Scheme of a possible double anticrossing between spin-paired level  $i$  and  $i+1$  (left, the black arrows indicate the spin), which could lead to the observed structure in the correlation for peaks c, d and e (right).

$$P_{int}^{\beta}(\bar{\xi}^*, \sigma_{\xi^*}) = \frac{1}{\sqrt{2\pi}\sigma_{\xi^*}} \left\{ \exp\left[-\frac{(s - \bar{\xi}^*)^2}{2\sigma_{\xi^*}^2}\right] + \exp\left[-\frac{s^2}{2\sigma_{\xi^*}^2}\right] \times P^{\beta}(s + \xi^*) \right\} \quad (2)$$

Here, the “ $\times$ ” denotes the convolution. Since  $\Delta$  is determined by the dot size and the material parameters, we can fit  $P_{int}^{\beta}(\bar{\xi}^*, \sigma_{\xi^*})$

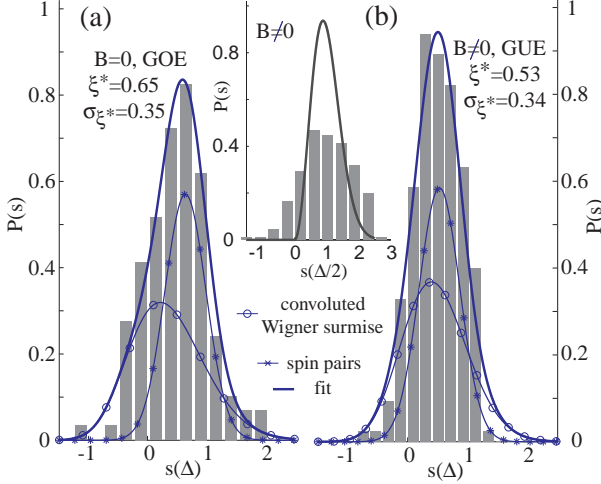


FIG. 3. Measured NNS distributions (gray bars) for  $B=0$  (a) and  $B \neq 0$  (b). The bold solid curves are the fits to  $P_{int}^{\beta}(\bar{\xi}^*, \sigma_{\xi^*})$ , with the fit results as indicated in the figure (see text). Also drawn are the two components of  $P_{int}^{\beta}$ , i.e. the Gaussian distribution of separations between spin pairs, and its convolution with the corresponding Wigner surmises. The inset compares the GUE data to  $P^2(s)$  (eq. 1), using the spin-resolved level spacing  $\Delta/2$  as the average peak separation.

to the measured NNS distribution with the two fit parameters  $\bar{\xi}^*$  and  $\sigma_{\xi^*}$  (Fig.3). We obtain  $\bar{\xi}^* = 0.65$  and  $\sigma_{\xi^*} = 0.35$  for GOE, as well as  $\bar{\xi}^* = 0.53$  and  $\sigma_{\xi^*} = 0.34$  for GUE. Hence, we find that  $\xi$  is higher for GOE than for GUE, which is in agreement with the theoretical prediction [22]. The fluctuation of  $\xi$  is found to be independent of the Gaussian ensemble, and does not vary continuously with  $B$ .

In these fits, we have assumed that two electrons are always successively filled in one spatial wave function, i.e. we have neglected situations in which  $\xi_i > \Delta_i$ . Inclusion of avoided crossings would require more clearly pronounced kinks than those in our data (sometimes the pair correlation is lost while a kink is not clearly visible). More experiments as well as theoretical work is necessary to investigate this dependence, also with respect to fluctuations in  $\xi$  with  $B$ .

Finally, we consider how our data can be modelled when complete absence of spin pairing is assumed. In this case, the mean level spacing would be  $\Delta/2$ . Comparing a correspondingly normalized Wigner surmise to our

data gives an extremely poor result (inset in Fig.3): the measured NNS distribution appears too wide by a factor of  $\approx 2$ .

In summary, we have observed spin pairing effects in a - compared to dots investigated in earlier experiments - rigid quantum dot with reduced electron-electron interactions. We have observed spin pairing which persists as a magnetic field is varied, but is interrupted by kinks as well as other structures in the parametric evolution of the Coloumb blockade peaks. We have extracted the average interaction energy  $\bar{\xi}$  between states of identical spatial wave functions but opposite spin. Furthermore, we explain the measured distributions of nearest neighbor spacings as being composed of the two branches of a modified, bimodal Wigner-Dyson distribution, which takes  $\bar{\xi}$  and its fluctuation into account.

It is a pleasure to thank H. U. Baranger, E. Mucciolo, K. Richter, and F. Simmel for stimulating conversations and discussions. Financial support from the Schweizerischer Nationalfonds is gratefully acknowledged.

---

- [1] For a review, see L.P. Kouwenhoven, C.M. Marcus, P.L. McEuen, S. Tarucha, R.M. Westervelt, and N.S. Wingreen, "Electron Transport in Quantum Dots", in Mesoscopic Electron Transport, Proceedings of a NATO Advanced Study Institute, edited by L.P. Kouwenhoven, G. Schön and L. L. Sohn, (Kluwer, Dordrecht, Netherlands, 1997), ser. E, vol. 345, pp. 105-214.
- [2] M.L. Mehta, Random Matrices, Academic Press, London(1991).
- [3] C.W.J. Beenakker, Rev. Mod. Phys. **69**, 731 (1997).
- [4] C. W. Beenakker, Phys. Rev. B **44**, 1646, (1991).
- [5] M.A. Kastner, Rev. Mod. Phys. **64**, 849, (1992).
- [6] U. Sivan, R. Berkovits, Y. Aloni, O. Prus, A. Auerbach, and G. Ben-Yoseph, Phys. Rev. Lett. **77**, 1123, (1996).
- [7] F. Simmel, T. Heinzel, and D. Wharam, Europhys. Lett. **38**, 123 (1997).
- [8] S.R. Patel, S.M. Cronenwett, D.R. Stewart, A.G. Huibers, C.M. Marcus, C.I. Duruöz, J.S. Harris Jr, K. Campman, and A.C. Gossard, Phys. Rev. Lett. **80**, 4522, (1998).
- [9] F. Simmel, D. Abusch-Magder, D. A. Wharam, M. A. Kastner, and J. P. Kotthaus, Phys. Rev. B **59**, R10441, (1999).
- [10] S.R. Patel, D.R. Stewart, C.M. Marcus, M. Gökcedak, Y. Alhassid, A.D. Stone, C.I. Duruöz, and J.S. Harris, Jr, Phys. Rev. Lett. **81**, 5900, (1998).
- [11] R. Berkovits and B.L. Altshuler, Phys. Rev. B **55**, 5297, (1997).
- [12] Y.M. Blanter, A.D. Mirlin, and B.A. Muzykantskii, Phys. Rev. Lett. **78**, 2449, (1997).
- [13] A. Cohen, K. Richter, and R. Berkovits, Phys. Rev. B **60**, 2536, (1999).

- [14] P. N. Walker, Y. Gefen, and G. Montambaux, Phys. Rev. Lett. **82**, 5329 (1999), and references therein.
- [15] K.-H. Ahn, K. Richter, and I.-H. Lee, cond-mat/9906046 (unpublished), and references therein.
- [16] Y. Alhassid, P. Jacquod, and A. Wobst, cond-mat/9909066 (unpublished), and references therein.
- [17] D.R. Stewart, D. Sprinzak, C.M. Marcus, C.I. Duruöz, and J.S. Harris Jr., Science **278**, 1784, (1997).
- [18] G. Hackenbroich, W.D. Weiss, and H.A. Weidenmüller, Phys. Rev. Lett. **79**, 127, (1997).
- [19] R.O. Vallejos, C.H. Lewenkopf, and E.R. Mucciolo, Phys. Rev. Lett. **81**, 677, (1998); R.O. Vallejos, C.H. Lewenkopf, and E.R. Mucciolo, Phys. Rev. B **60**, 13682 (1999).
- [20] R. Held, T. Vancura, T. Heinzel, K. Ensslin, M. Holland, and W. Wegscheider, Appl. Phys. Lett. **75**, 1134 (1999); R. Held, S. Lüscher, T. Heinzel, K. Ensslin, and W. Wegscheider, *ibid.* **75**, 1134 (1999); S. Lüscher, A. Fuhrer, R. Held, T. Heinzel, K. Ensslin, and W. Wegscheider, *ibid.* **75**, 2452 (1999).
- [21] A simple image charge calculation reveals that the top gate reduces  $r_s$  only by  $\approx 2\%$ . Nevertheless, it improves screening of impurity potentials and the confining potential becomes steeper.
- [22] H. U. Baranger, D. Ullmo, L. I. Glazman, cond-mat/9907151.
- [23] D. Goldhaber-Gordon, H. Shtrikman, D. Mahalu, D. Abusch-Magder, U. Meirav, and M.A. Kastner, Nature **391**, 156 (1998).
- [24] S. M. Maurer, S. R. Patel, C. M. Marcus, C. I. Duruöz, J. S. Harris, Jr. Phys. Rev. Lett. **83**, 1403, (1999).
- [25] H.U. Baranger, private communication (2000)